Synthesis, Structure, and Electrical Properties of a New Family of Mixed-Metal Sulfides Containing Rutile-like $[InS_4]_\infty/[TiS_4]_\infty$ Chains: $(RE)_6In_{1-x}Ti_{1+x}S_{12}$ (RE = Nd, Sm, Gd)

Yi-Chung Hung and Shiou-Jyh Hwu*,†

Department of Chemistry, Rice University, P.O. Box 1892, Houston, Texas 77251

Received March 20, 1995. Revised Manuscript Received June 13, 1995[⊗]

Via iodine vapor-flux reactions, single crystals of a new family of mixed-metal sulfides in the pseudoternary $(RE)_2S_3-In_2S_3-Ti_2S_3$ systems were isolated. The general formula of these phases can be written as $(RE)_6In_{1-x}Ti_{1+x}S_{12}$, where RE/$x$ = Nd/0.22 (**1**), Sm/0.16 (**2**), Gd/0.26 (**3**), and Gd/0.86 (**4**); $Z = 2$. The single-crystal X-ray diffraction studies showed that these sulfides crystallize in the *Pnnm* (No. 58) space group. The cell constants are as follows: **1**: a = 13.716 (2) Å, b = 16.267 (2) Å, c = 3.917 (2) Å, V = 873.9 (3) Å^3; **2**: a = 13.597 (3) Å, b = 16.200 (2) Å, c = 3.857 (3) Å, V = 849.7 (7) Å^3; **3**: a = 13.530 (2) Å, b = 16.265 (4) Å, c = 3.854 (4) Å, V = 848 (1) Å^3; **4**: a = 13.429 (8) Å, b = 16.109 (6) Å, c = 3.785 (8) Å, V = 819 (2) Å^3. The title compounds are isostructural with Sm_3InS_6, where the two crystallographically independent indium sites are substituted in a preferential manner by titanium(III) cations. The frameworks are quasi-one-dimensional resulting from a juxtaposition of $[InS_4]_\infty/[TiS_4]_\infty$ chains. The parallel chains are interconnected by rare-earth cations, $(RE)^{3+}$. The nearest Ti–Ti interaction corresponds to the shortest crystallographic axis, i.e., $d_{Ti-Ti} \equiv c$, across shared edges of octahedra. Four-probe resistivity measurements on single crystals show a simple semiconducting behavior with a slight departure toward an insulating state at low temperatures. A brief discussion about the electronic behavior and its correlation with the structure is presented.

Introduction

One-dimensional (1D) conductors are of fundamental interest in studying unusual physical phenomena, such as metal–insulator (M–I) transitions and charge density waves (CDW), which are associated with electron–electron and electron–phonon interactions.[1] Peierls[2] suggests that at $T = 0$ K, no 1D solid is metallic because of the structural distortion through which the metallic electrons are localized. A classic example is demonstrated by the mixed-valence Krogmann salt, $K_2Pt(CN)_4Br_{0.30}{\cdot}xH_2O$ (KCP), a coordination solid whose structure contains staggered square-planar $Pt(CN)_4$ units stacked to form linear chains of platinum atoms.[3] This compound exhibits one-dimensional metallic properties with a M–I transition due to a structural phase transition resulting in alternating long-and-short Pt–Pt bonds below the critical temperature. MQ_3 and $(MQ_4)_nX$ (M = Nb, Ta; Q = S, Se; X = halogen) are two novel families of extended solids that possess interesting CDW phenomena.[4] These pseudo-one-dimensional tri- and tetrachalcogenide structures are comparable to KCP in two ways, as far as the nature of CDW is concerned: (i) significant 1D M–M interactions with d_{z^2} orbital overlap; (ii) weak interchain coupling. The latter may be responsible for the lattice instabilities that give rise to the observed CDW. It is thought that the M–I transition may be suppressed and 1D metallic properties may be extended if a conducting chain is embedded in a rigid 3D framework where energy-driven structural distortion may be less favorable. The title compounds provide an interesting structural family for the discussion of such a proposal.

Knowledge of the structures of indium-based chalcogenides implies that the desired structural features with regard to rigid-1D transition-metal chalcogenide chains may be acquired via chemical substitution of In^{3+} with trivalent transition metal cations, Ti^{3+} in this case. In the $(RE)_2S_3-In_2S_3$ (RE = La–Yb) systems, for example, Guittard and co-workers[5] have reported a large family of interesting solids with complicated structural types that all contain edge-shared InS_6 octahedral chains.[6–9] These are $(RE)_3InS_6$ (RE = La–Nd, orthorhombic $P2_12_12$, La_3InS_6-type;[6] RE = Sm–Tb, orthorhombic *Pnnm*, Sm_3InS_6-type[7]), $(RE)InS_3$ (RE = La–Nd, unknown space group), $(RE)_3In_5S_{12}$ (RE = Sm–Tb, monoclinic $P2_1/m$, $Tb_3In_5S_{12}$-type),[8] and $(RE)_xIn_{8/3-x}S_4$ (RE = Dy–Yb, cubic spinel).[9] In 1979, Guseinov and co-workers[10] reported a new structural type with the composition of $Nd_4In_{5-x}S_{13}$, which crystallizes in space

† Permanent address: Department of Chemistry, Clemson University, Clemson, SC 29634.

⊗ Abstract published in *Advance ACS Abstracts,* July 15, 1995.

(1) (a) Miller, J. S.; Epstein, A. J. In *Progress in Inorganic Chemistry*; Lippard, S. J., Ed.; John Wiley & Sons, Inc.: New York, 1976; Vol. 20, p 1. (b) Rouxel, J. In *Crystal Chemistry and Properties of Materials with Quasi-One-Dimensional Structures*, Rouxel, J., Ed.; D. Reidel Publishing Co.: Boston, 1986; p 1.

(2) Peierls, R. E. In *Quantum Theory of Solids*; Clarendon Press: Oxford, 1955.

(3) Comés, R.; Lambert, M.; Launois, H.; Zeller, H. R. *Phys. Rev.* **1973**, *B8*, 571.

(4) Meerschaut, A.; Rouxel, J. In *Crystal Chemistry and Properties of Materials with Quasi-One-Dimensional Structures*; Rouxel, J., Ed.; D. Reidel Publishing Co.: Boston, 1986; p 205 and references therein.

(5) Guittard, M.; Carré, D.; Kabré, T. S. *Mater. Res. Bull.* **1978**, *13*, 279.

(6) Carré, D.; Guittard, M.; Adolphe, C. *Acta Crystallogr.* **1978**, *B34*, 3499.

(7) Messain, D.; Carré, D.; Laruelle, P. *Acta Crystallogr.* **1977**, *B32*, 2540.

(8) Carré, D. *Acta Crystallogr.* **1977**, *B33*, 1163.

(9) Karayev, Z.; Keiserukhskaya, L.; Aliyeva, Sh.; Gadymov, A. *Azerb. Khim. Zh.* **1966**, *1*, 112.

0897-4756/95/2807-1661$09.00/0

Table 1. Crystallographic Data[a] for $(RE)_6In_{1-x}Ti_{1+x}S_{12}$

	1	2	3	4
chemical formula	$Nd_6In_{1-x}Ti_{1+x}S_{12}$ ($x = 0.22$)	$Sm_6In_{1-x}Ti_{1+x}S_{12}$ ($x = 0.16$)	$Gd_6In_{1-x}Ti_{1+x}S_{12}$ ($x = -0.26$)	$Gd_6In_{1-x}Ti_{1+x}S_{12}$ ($x = 0.86$)
formula weight (amu)	1398.16	1439.13	1508.34	1433.39
a, Å	13.716 (2)	13.597 (3)	13.530 (2)	13.429 (8)
b, Å	16.267 (2)	16.200 (2)	16.265 (4)	16.109 (6)
c, A	3.917 (2)	3.857 (3)	3.854 (4)	3.785 (8)
V, Å^3	873.9 (3)	849.6 (7)	848 (1)	819 (2)
Z	2	2	2	4
space group	*Pnnm* (No. 58)	*Pnnm* (No. 58)	*Pnnm* (No. 58)	*Pnnm* (No. 58)
T, °C	23	23	23	23
λ, Å	0.71069	0.71069	0.71069	0.71069
ϱ_{calcd}, g cm^{-3}	5.316	5.628	5.909	5.815
linear abs. coeff, cm^{-1}	204.46	234.92	266.40	265.56
R[b]	0.020	0.029	0.025	0.029
R_w[c]	0.031	0.035	0.034	0.051

[a] The refinement of cell constants is constrained in the orthorhombic crystal system. [b] $R = \Sigma[|F_o| - |F_c|] / |\Sigma|F_o|$. [c] $R_w = [\Sigma w[|F_o| - |F_c|]^2 / \Sigma w|F_o|^2]^{1/2}$.

group *Pbam* of the orthorhombic system. Additionally, two other compound families, $(RE)In_3S_6$ (RE = La−Er) and $(RE)In_2S_4$ (RE = Eu−Yb), have been known since 1980.[11] Compared to the large number of indium compounds, only three compounds in the pseudobinary $(RE)_2S_3-Ti_2S_3$ systems have been reported thus far, $(RE)TiS_3$ (RE = La, Sm, Tb),[12] and none in the $In_2S_3-Ti_2S_3$ system.

During our exploratory synthesis of mixed-metal chalcogenide compounds in the $(RE)InS_3-(RE)TiS_3$ (RE = Nd, Sm, Gd) systems, four new quaternary compounds that adopt the Sm_3InS_6-type structure were synthesized with the general formula $(RE)_6In_{1-x}Ti_{1+x}S_{12}$. A different phase adopting a new structural type was also isolated, e.g., $Nd_{14}InTi_3S_{28}$.[13] In this report we present the synthesis, X-ray single-crystal structure, electrical properties, and qualitative band structure of the new family of quasi-one-dimensional, mixed-metal sulfides.

Experimental Section

Precursor Synthesis and Single-Crystal Growth. Single crystals of the title compounds were prepared using a two-step synthetic method. The first step of the synthesis entailed the preparation of quaternary compound mixtures with conventional high-temperature solid-state reactions. Rare-earth metals (RE = Nd, Sm, Gd; Aesar or Aldrich 99.9%), In (Aldrich, 99.999%), Ti (Aldrich, 99.9%) and S (Aldrich, 99.99%) powders were used as reactants. A mixture of ca. 0.5 g of RE, In, Ti, and S with the nominal composition of $(RE)_2InTiS_6$ was ground under a blanket of nitrogen in a drybox and then loaded into a quartz ampule. The ampule was sealed under vacuum. The reaction mixtures were heated stepwise to avoid explosion due to volatile sulfur to a final temperature of 1100 °C, where the reaction was annealed for 4 days to achieve an intimate mixing. The final product was quenched in air and subject to examination by powder X-ray diffraction methods (showing no identifiable phases) prior to being employed as charge material for crystal growth.

The second-step single-crystal growth reaction was performed in a quartz ampoule containing the prereacted materials via an iodine vapor-flux method. The charge (~0.5 g) was loaded in the ampoule (~5 cm^3) with a small amount of I_2 (~40 mg). The reaction was carried out by heating with a temperature gradient between 995 and 895 °C for 6 days and furnace cooled to room temperature. Black shiny needle crystals of the title compounds were isolated as the major product from the high-temperature end of the tube. A second phase was identified as a misfit-layer compound $(RE)TiS_3$ at the low-temperature end,[13,14] and in one system the above-mentioned $Nd_{14}InTi_3S_{28}$ phase was present in addition to these phases. Qualitative elemental analysis of all single crystalline samples was carried out by energy dispersive spectroscopy (EDS). The results indicated the presence of all four elements. All the compounds seem stable in air at room temperature. Stoichiometric synthesis of Nd_6InTiS_{12} was performed with a method similar to that used in step one of the experimental procedure.

X-ray Single-Crystal Structure Determination. All four phases were examined with a Rigaku AFC5S four-circle X-ray diffractometer equipped with a graphite monochrometer. The crystallographic data are summarized in Table 1. Unless otherwise noted, for convenience of discussion, detailed crystallographic examination procedures only for the Nd_6InTiS_{12} phase are presented herein. Structure determination of Nd_6InTiS_{12} was performed on a 0.05 × 0.05 × 0.5 mm single crystal. The data collection procedures were the same as previously reported.[15] The unit-cell parameters and the orientation matrix for data collection were determined by a least-squares fit of 25 reflections ($10.21° \le 2\theta \le 17.99°$) and refined in the orthorhombic crystal system with 25 high-angle reflections ($30.17° \le 2\theta \le 36.33°$). The intensities of three standard reflections (0,−1,−1; 2,−4,0; 1,−4,0) were measured every 150 reflections. No significant intensity variation was observed during the course of data collection. The TEXSAN software package[16] was used for crystal structure solutions and refinements. Data reduction and intensity analysis were accomplished with the program PROCESS. On the basis of the intensity statistics as well as the successful solution and structure refinements, the space group was determined to be *Pnnm* (No. 58). Lorentz−polarization and empirical absorption corrections, based on three selected azimuthal scans (2θ = 11.94°, 24.01°, and 10.71°), were applied to the intensity data. The atomic coordinates were found by direct methods with the program SHELXS.[17] The structural and anisotropic thermal parameters were refined by full-matrix least-squares methods based on the structural formula "Nd_6InTiS_{12}" to R = 0.034, R_w = 0.057, and GOF = 2.43. After the initial stages of refinement, disordering on In and Ti sites was suggested by the abnormal thermal parameters. The occupancy factors for all the atoms in the structure were initially refined, but the resultant values indicated nonstoichiometry only on the indium and titanium sites. The refined multiplicities for the indium and titanium atoms were 0.207(1) and 0.278(2), respectively. An inclusion of the secondary extinction[18] into

(10) Guseinov, G.; Mamedov, F.; Shnulin, A.; Mamedov, Kh. *Dohl. Akad. Nauk SSSR* **1979**, *246*, 1360.
(11) Aliev, O. M. *Izv. Akad. Nauk SSSR, Ser. Neorg. Mater.* **1980**, *16*, 1514.
(12) Donohue, P. C. *J. Solid State Chem.* **1975**, *12*, 80.
(13) Hung, Y.-C. Ph.D. Dissertation, Rice University, 1994.
(14) Hung, Y.-C. *Inorg. Chem.* **1993**, *32*, 5427.
(15) Carpenter, J. D.; Hwu, S.-J. *Chem. Mater.* **1992**, *4*, 1368.
(16) TEXSAN: Single Crystal Structure Analysis Software, version 5.0. Molecular Structure Corp., The Woodlands, TX, 1989.
(17) Sheldrick, G. M. In *Crystallographic Computing 3*; Sheldrick, G. M., Krüger, C., Goddard, R., Eds.; Oxford University Press: London, 1985; pp 175−189.
(18) Zachariasen, W. H. *Acta Crystallogr.* **1968**, *A24*, 212.

Table 2. Atomic Coordinates and Thermal Parameters[a] for $Nd_6In_{1-x}Ti_{1+x}S_{12}$, $x = 0.22$

atom	x	y	z	B_{eq}, Å^2
Nd(1)	0.45101 (3)	0.21734 (3)	1/2	0.61 (2)
Nd(2)	0.23932 (4)	0.39947 (3)	1/2	0.74 (2)
Nd(3)	0.18183 (3)	0.14906 (3)	0	0.61 (2)
In[b]	0	0	1/2	0.79 (5)
Ti[b]	0	1/2	1/2	0.87 (9)[c]
S(1)	0.0853 (2)	0.4251 (1)	0	0.77 (8)
S(2)	0.3132 (2)	0.2882 (1)	0	0.76 (8)
S(3)	0.1025 (2)	0.2531 (1)	1/2	0.69 (8)
S(4)	0.3782 (2)	0.1038 (1)	0	0.87 (8)
S(5)	0.1865 (2)	0.0213 (1)	1/2	0.69 (8)
S(6)	0.4774 (2)	0.3969 (1)	1/2	0.89 (8)

[a] Anisotropically refined atoms are given in the form of the isotropic equivalent displacement parameters defined as $B_{eq} = (8\pi^2/3)$ trace U. [b] The multiplicities were first refined with fixed thermal parameters. The multiplicities of In/Ti on the In and Ti sites were fixed for the final refinement, i.e., 0.175/0.075 and 0.021/0.229 for In and Ti sites, respectively (see text). [c] With a fixed occupancy factor, the refined thermal parameter B_{eq} of Ti is negatively definite.

the last stage of structural refinement reduced the number of reflections that had $\Delta F/\sigma F > 20$ from 12 to 5 and in turn improved the R/R_w from 0.027/0.040 to 0.020/0.031. Subsequent least-squares refinements resulted in a final structure solution to GOF = 1.31 based on F. On the basis of nonstoichiometry, both indium and titanium sites were intuitively considered as mixed In/Ti sites, and the calculated structural formula was $Nd_6(In_{0.70}/Ti_{0.30})(In_{0.08}/Ti_{0.92})S_{12} \equiv Nd_6In_{1-x}Ti_{1+x}S_{12}$ ($x \sim 0.22$) (**1**). The nonstoichiometry was found in the three other title compounds. The refined structural formulas were $(RE)_6In_{1-x}Ti_{1+x}S_{12}$, where RE/$x$ = Sm/0.16 (**2**), Gd/−0.26 (**3**), and Gd/0.86 (**4**). The final fractional atomic coordinates and thermal parameters for **1** are listed in Table 2, while those of other phases are listed in Table SII of supporting information.

Wavelength-Dispersive Spectroscopy (WDS) Analysis. The structural composition of **1** was confirmed by wavelength dispersive spectroscopy. A Cameca SX-50 electron microprobe was employed for the analysis. The acceleration voltage was set at 15 keV; the specimen current was adjusted to 15 nA; and the counting times were 20 s for both the standards and the samples. Data acquisition was accomplished using four scanning spectrometers. The intensities of each of the X-ray emissions of the sample were compared with those of a standard. The standards used for the analysis were rare-earth glass standard no. 2,[19] InAs (Tousimis), pure Ti metal, and Pyrite (Tousimis). The normalized ratio was Nd:In:Ti:S = 6.3:0.9:1.0:12, consistent with that derived from the structural formula, 6.0:0.8:1.2:12.

Powder X-ray Diffraction. The stoichimetric compound Nd_6InTiS_{12} was prepared in a polycrystalline form and was subsequently analyzed by powder X-ray diffraction methods.[15] The diffraction patterns were indexed and refined by the least-squares program LATT.[19] NIST (National Institute of Standards and Technology) silicon powder was used as an internal standard. Thirty-one reflections were used in refinements giving the cell parameters: $a = 13.701(3)$ Å, $b = 16.282(4)$ Å, $c = 3.922(1)$ Å, and $V = 874.9(4)$ Å^3, which are in a relatively good agreement with the parameters from single crystal indexing. The small difference is attributed to the nonstoichiometry with respect to the In/Ti composition revealed in the above structural analysis.

Differential Thermal Analysis (DTA). The DTA of **1** was performed on a ground sample of selected single crystals (~15 mg) using the procedures previously described.[21] Neither a phase transition nor melting phenomena were observed up to ~1250 °C.

Electrical Property Measurements. Variable-temperature resistivity measurements of the single crystals of $(RE)_6InTiS_{12}$ (RE = Nd, Sm, and Gd) and Gd_3TiS_6 were conducted using previously described procedures.[22] The crystals were typically between 1 and 3 mm in length and approximately rectangular with a cross section of about 0.07 × 0.07 mm. Because of the size limitation, only the measurements parallel to the needle axis c were performed. For phase confirmation, single crystals were examined by X-ray single-crystal methods. On the basis of closest volume comparison, the formula of each phase is represented by nearest integers for the convenience of discussion. The indexed cell constants listed below are not precisely consistent with those in Table 1; this is because of nonstoichiometry with respect to the In/Ti composition:

	a (Å)	b (Å)	c (Å)	V (Å^3)
Nd_6InTiS_{12}	13.719 (5)	16.269 (10)	3.917 (2)	874.2 (8)
Sm_6InTiS_{12}	13.616 (2)	16.200 (2)	3.8798 (9)	857.5 (3)
Gd_6InTiS_{12}	13.545 (6)	16.256 (10)	3.856 (5)	848 (1)
Gd_3TiS_6	13.431 (7)	16.093 (10)	3.805 (2)	822.4 (8)

Results and Discussion

Structure Description. This new family of quaternary sulfides, $(RE)_6In_{1-x}Ti_{1+x}S_{12}$, is isostructural with Sm_3InS_6 ($\equiv Sm_6InInS_{12}$), in which the octahedrally coordinated indium sites are partially substituted by the trivalent titanium cations. Detailed structural analysis suggests that one of the indium sites is preferentially occupied by titanium. The structural formula of **1**, for example, can be written as $Nd_6(In_{0.70}/Ti_{0.30})(In_{0.08}/Ti_{0.92})S_{12}$. The resulting preferred occupancy, as opposed to a statistical distribution, is consistent with what appears to be the reason that the title compounds adopt the Sm_3InS_6-type structure instead of the La_3InS_6-type. The latter differs from the former by its coordination environments with respect to indium, e.g., one InS_4 tetrahedral site and one InS_6 octahedral site. The Sm_3InS_6-type structure has two distinct InS_6 octahedral sites, one more distorted than the other. While both sites in this structural type are susceptible to Ti^{3+} substitution, it is recognized that the Ti-dominating octahedral site coincides with the distorted InS_6 in the parent structure. This distortion facilitates the preferred substitution for the Jahn−Teller cation Ti^{3+} (d^1, through hole formalism). It should be noted that the selective substitution is accompanied by a small degree of random distribution, as exemplified by phase **3**, $Gd_6In_{1.26}Ti_{0.74}S_{12} \equiv Gd_6(In_{0.81}Ti_{0.19})(In_{0.45}Ti_{0.55})S_{12}$, where both octahedral sites are partially substituted even though the total occupancy level of Ti is less than 50%.

The title compounds crystallize in a pseudo-one-dimensional framework. The ORTEP[23] drawing in Figure 1 shows a perspective view of the unit cell of an idealized Nd_6InTiS_{12} structure, where the preferred site is labeled as Ti and the other is In. The structure is viewed down along the c axis, parallel to the InS_6 (thin bonds) and TiS_6 (thick bonds) octahedral chains. The indium and titanium atoms occur on the mirror planes at $z = 0$ and $z = 1/2$. The fused InS_6 and TiS_6 octahedra form rutile-like chains extending along the [001] direction by sharing opposite edges, giving rise to structural formulae $[InS(6)_{4/2}S(5)_{2}]_\infty \equiv [InS_4]_\infty$ and $[TiS(1)_{4/2}S(4)_{2}]_\infty \equiv [TiS_4]_\infty$, respectively. The trivalent neodymium cations, as shown in cross-hatched circles, are located

(19) Drake, M. J.; Weill, D. F. *Chem. Geol.* **1972**, *10*, 179.
(20) LATT: F. Takusagawa, Ames Laboratory, Iowa State University, Ames, IA, unpublished research, 1981.
(21) Bucher, C. K.; Hwu, S.-J. *Inorg. Chem.* **1994**, *33*, 5831.
(22) Wang, S.; Hwu, S.-J. *Inorg. Chem.* **1995**, *34*, 166.
(23) Johnson, C. K. *ORTEP II*; Report ORNL-5138; Oak Ridge National Laboratory: Oak Ridge, TN, 1976.

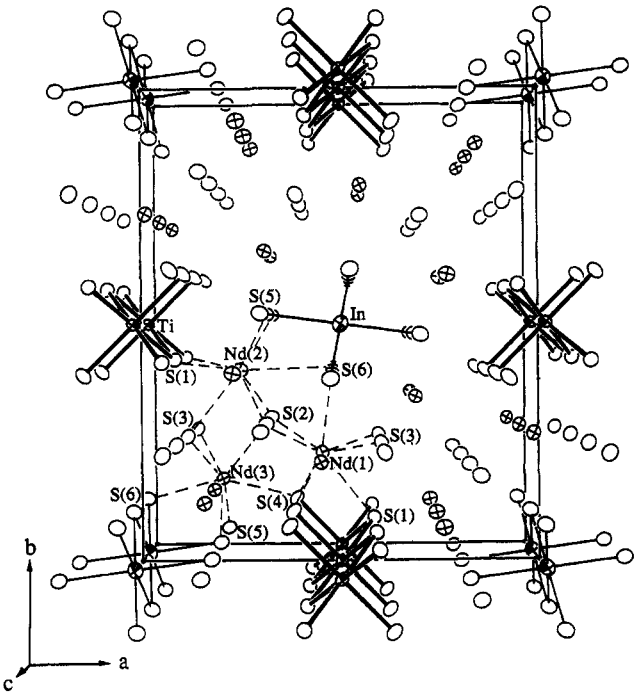

Figure 1. Perspective view of an idealized Nd_6InTiS_{12} structure. The $[InS_4]_\infty$ and $[TiS_4]_\infty$ chains are outlined by thin and thick lines, respectively. The cross-hatched circles are Nd^{3+} cations, whose connectivity to the rutile-like chains is outlined by dotted lines. The anisotropic atoms are presneted at 90% probability.

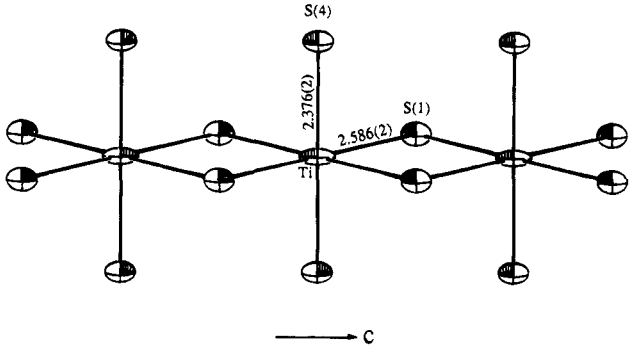

Figure 2. ORTEP drawing of the edge-shared $[TiS_4]_\infty$ chain. The anisotropic atoms are presented at 90% probability. The bond distances are in angstroms.

between the infinite chains to interconnect InS_6 and TiS_6 octahedra. The coordination of three crystallographically independent neodymium atoms is outlined by dashed lines.

Table 3 lists bond distances and angles concerning the coordination geometries of the cation-centered sulfur polyhedra in structure **1**. The 90° octahedral angles for InS_6 and TiS_6 units are in the range of 82.1°−97.9° and 81.6°−98.4°, respectively, indicating that both octahedral environments are slightly distorted. The Ti−S bonds consist of two short Ti−S(4) apical bonds, 2.376 (2) Å, and four long Ti−S(1) equatorial bonds, 2.586 (2) Å, as shown in Figure 2. The observed distortion is consistent with the Jahn−Teller effect due to the Ti^{3+} (d^1) cation.[24] The corresponding In site of the Sm_3InS_6 structure presents a similar distortion, e.g., 2.43/2.72 Å, respectively. In any event, the average Ti−S bond distance, 2.52 Å, is comparable with the sum of Shannon crystal radii, 2.51 Å, of the 6-coordinated Ti^{3+} (0.81 Å)

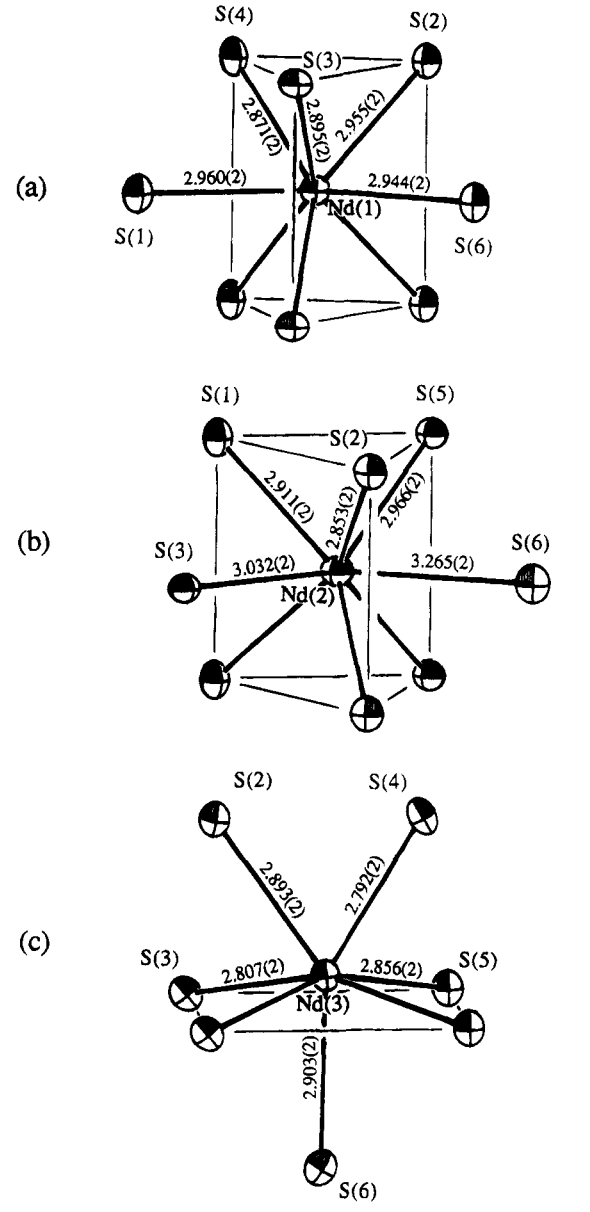

Figure 3. ORTEP drawings of (a) $Nd(1)S_8$, (b) $Nd(2)S_8$, and (c) $Nd(3)S_7$ polyhedra. The lines between sulfurs are drawn to show the polyhedra described in the text. The anisotropic atoms are presneted at 90% probability. The bond distances are in angstroms.

and S^{2-} (1.70 Å).[25] The In−S bond distances for the InS_6 octahedron are relatively homogeneous, e.g., 2.582−2.597 Å. These are slightly shorter than 2.61 Å, the average In−S bond distance in Sm_3InS_6, and 2.64 Å, the sum of Shannon crystal radii for the 6-coordinated In^{3+} (0.94 Å) and S^{2-} (1.70 Å). This is most likely due to the partial substitution of a smaller cation Ti^{3+}.

The three crystallographically independent neodymium cations are seven- or eight-coordinate with respect to the sulfur anions. Two of them, Nd(1) and Nd(2), adopt 8-fold coordination as shown in Figure 3a,b, respectively, while Nd(3) has a 7-fold coordination

(24) For the title compounds, the average bond distances (angstroms) of In−S/Ti−S and the absolute difference between long and short bonds of $\Delta d_{In-S}/\Delta d_{Ti-S}$ are: **1**, 2.591/2.516, 0.013/0.210; **2**, 2.570/2.500, 0.006/0.205; **3**, 2.581/2.550, 0.003/0.233; **4**, 2.497/2.476, 0.037/0.175, respectively. It is noted that the Jahn−Teller effect in **4** is apparent for both In/Ti sites due to high Ti occupancy on the otherwise In site, e.g., $Gd_6(In_{0.14}Ti_{0.86})TiS_{12}$.

(25) Shannon, R. D. *Acta Crystallogr.* **1976**, *A32*, 751.

Table 3. Selected Bond Distances (Å) and Angles (deg) for $Nd_6In_{1-x}Ti_{1+x}S_{12}$, $x = 0.22$

		$Nd(1)S_8$	
Nd(1)–S(1)[g]	2.960 (2)	Nd(1)–S(4)[a,c]	2.871 (2) (2×)
Nd(1)–S(2)[a,c]	2.955 (2) (2×)	Nd(1)–S(6)[a]	2.944 (2)
Nd(1)–S(3)[g,j]	2.895 (2) (2×)		
S(1)[g]–Nd–S(2)[a,c]	134.67 (4) (2×)	S(2)[a/c]–Nd–S(4)[c/a]	118.70 (6) (2×)
S(1)[g]–Nd–S(3)[g,j]	71.56 (5) (2×)	S(2)[a,c]–Nd–S(6)[a]	72.04 (5) (2×)
S(1)[g]–Nd–S(4)[a,c]	73.32 (5) (2×)	S(3)[g]–Nd–S(3)[j]	85.12 (6)
S(1)[g]–Nd–S(6)[a]	134.47 (6)	S(3)[g/j]–Nd–S(4)[a/c]	83.99 (5) (2×)
S(2)[a]–Nd–S(2)[c]	83.01 (6)	S(3)[g/j]–Nd–S(4)[c/a]	144.88 (6) (2×)
S(2)[a/c]–Nd–S(3)[g/j]	86.89 (5) (2×)	S(3)[g,j]–Nd–S(6)[a]	75.33 (5) (2×)
S(2)[a/c]–Nd–S(3)[j/g]	147.37 (6) (2×)	S(4)[a]–Nd–S(4)[c]	86.01 (6)
S(2)[a/c]–Nd–S(4)[a/c]	64.93 (5) (2×)	S(4)[a,c]–Nd–S(6)[a]	132.93 (4) (2×)
		$Nd(2)S_8$	
Nd(2)–S(1)[a,c]	2.911 (2) (2×)	Nd(2)–S(5)[k,n]	2.966 (2) (2×)
Nd(2)–S(2)[a,c]	2.853 (2) (2×)	Nd(2)–S(6)[a]	3.265 (2)
Nd(2)–S(3)[a]	3.032 (2)		
S(1)[a]–Nd–S(1)[c]	84.57 (6)	S(2)[a,c]–Nd–S(3)[a]	73.83 (5) (2×)
S(1)[a/c]–Nd–S(2)[a/c]	83.51 (5) (2×)	S(2)[a/c]–Nd–S(5)[k/n]	81.32 (5) (2×)
S(1)[a/c]–Nd–S(2)[c/a]	144.14 (6) (2×)	S(2)[a/c]–Nd–S(5)[n/k]	139.06 (6) (2×)
S(1)[a/c]–Nd–S(3)[a]	70.32 (5) (2×)	S(2)[a,c]–Nd–S(6)[a]	68.70 (5) (2×)
S(1)[a/c]–Nd–S(5)[k/n]	73.08 (5) (2×)	S(3)[a]–Nd–S(5)[k,n]	137.48 (3) (2×)
S(1)[a/c]–Nd–S(5)[n/k]	126.68 (6) (2×)	S(3)[a]–Nd–S(6)[a]	127.52 (6)
S(1)[a,c]–Nd–S(6)[a]	136.68 (3) (2×)	S(5)[k]–Nd–S(5)[n]	82.63 (6)
S(2)[a]–Nd–S(2)[c]	86.68 (6)	S(5)[k,n]–Nd–S(6)[a]	70.47 (5) (2×)
		$Nd(3)S_7$	
Nd(3)–S(2)[a]	2.893 (2)	Nd(3)–S(5)[a,b]	2.856 (2) (2×)
Nd(3)–S(3)[a,b]	2.807 (2) (2×)	Nd(3)–S(6)[h]	2.903 (2)
Nd(3)–S(4)[a]	2.792 (2)		
S(2)[a]–Nd–S(3)[a,b]	76.71 (5) (2×)	S(3)[a/b]–Nd–S(5)[b/a]	157.74 (6) (2×)
S(2)[a]–Nd–S(4)[a]	66.75 (6)	S(3)[a,b]–Nd–S(6)[h]	77.34 (5) (2×)
S(2)[a]–Nd–S(5)[a,b]	123.71 (5) (2×)	S(4)[a]–Nd–S(5)[a,b]	77.66 (5) (2×)
S(2)[a]–Nd–S(6)[h]	143.48 (6)	S(4)[a]–Nd–S(6)[h]	149.77 (6)
S(3)[a]–Nd–S(3)[b]	88.46 (6)	S(5)[a]–Nd–S(5)[b]	86.58 (6)
S(3)[a,b]–Nd–S(4)[a]	122.20 (5) (2×)	S(5)[a,b]–Nd–S(6)[h]	80.46 (5) (2×)
S(3)[a/b]–Nd–S(5)[a/b]	88.21 (5) (2×)		
		InS_6[o]	
In–S(5)[a,d]	2.582 (2) (2×)	In–S(6)[h,i,l,m]	2.597 (2) (4×)
S(5)[a]–In–S(5)[d]	180.00	S(6)[h/l]–In–S(6)[i/m]	97.92 (7) (2×)
S(5)[a/a/d/d]–In–S(6)[h/i/l/m]	91.82 (6) (4×)	S(6)[h/i]–In–S(6)[l/m]	82.08 (7) (2×)
S(5)[a/a/d/d]–In–S(6)[l/m/h/i]	88.18 (6) (4×)	S(6)[h/i]–In–S(6)[m/l]	180.00 (2×)
		TiS_6[o]	
Ti–S(1)[a,c,e,f]	2.586 (2) (4×)	Ti–S(4)[k,h]	2.376 (2) (2×)
S(1)[a/e]–Ti–S(1)[c/f]	98.44 (7) (2×)	S(1)[a/c]–Ti–S(1)[e/f]	81.56 (7) (2×)
S(1)[a/c/e/f]–Ti–S(4)[k/k/h/h]	90.96 (6) (4×)	S(1)[a/c]–Ti–S(1)[f/e]	180.00 (2x)
S(1)[a/c/e/f]–Ti–S(4)[h/h/k/k]	89.04 (6) (4×)	S(4)[k]–Ti–S(4)[h]	180.00

[a] x, y, z. [b] $x, y, -1 + z$. [c] $x, y, 1 + z$. [d] $-x, -y, z$. [e] $-x, 1 - y, z$. [f] $-x, 1 - y, 1 + z$. [g] $1/2 + x, 1/2 - y, 1/2 - z$. [h] $-1/2 + x, 1/2 - y, 1/2 - z$. [i] $-1/2 + x, 1/2 - y, 3/2 - z$. [j] $1/2 + x, 1/2 - y, 3/2 - z$. [k] $1/2 - x, 1/2 + y, 1/2 - z$. [l] $1/2 - x, -1/2 + y, 1/2 - z$. [m] $1/2 - x, -1/2 + y, 3/2 - z$. [n] $1/2 - x, 1/2 + y, 3/2 - z$. [o] $(In_zTi_{1-z})S_6$ octahedra: $z = 0.700$ and 0.084 for InS_6 and TiS_6, respectively.

(Figure 3c). The geometry of the $Nd(1)S_8$ and $Nd(2)S_8$ polyhedra can be best described as a bicapped trigonal prism (bTP), in which a trigonal prism is formed by six sulfur atoms with each of the two outer-sphere sulfurs, situated in the same mirror plane as the neodymium, capping two of the three lateral square faces of the prism. Each of these two outer-sphere Nd–S interactions is roughly perpendicular to the lateral face. The $Nd(3)S_7$ adopts a relatively distinct geometry which will be described later.

The two bTP NdS_8 polyhedra can be distinguished by the relationship of the Nd–S bond distances between the neodymium center and the vertex vs capping sulfur atoms (Table 3). Normally, the capping sulfur assumes a longer bond distance which suggests a weaker electrostatic interaction with the neodymium cation center. The two capping sulfur atoms can be viewed as the "outer-sphere" coordinates as compared to the vertex sulfur atoms of the trigonal prism. For example, in $Nd(2)S_8$, the Nd(2)–S(3) and Nd(2)–S(6) capping distances, 3.03–3.27 Å, are longer than the Nd(2)–S(1), Nd(2)–S(2), and Nd(2)–S(5) vertex distances, 2.85–2.97 Å. On the other hand, the capping sulfurs in $Nd(1)S_8$ adopt relatively short Nd–S distances, 2.94 and 2.96 Å, which lead to wider lateral faces. The ratio of long and short rectangular edges is 1.11 for the S(2)S(3)S(3)S(2) plane, while others are 1.02–1.03. In any event, the bTP geometry is a commonly seen structural feature and the average Nd–S distances (2.92 and 2.97 Å for Nd(1) and Nd(2) btps, respectively) are comparable with 2.949 Å, the sum of Shannon crystal radii of the eight-coordinated neodymium, Nd^{3+} (1.249 Å) and sulfur, S^{2-} (1.70 Å).

The third neodymium atom, Nd(3), has an interesting 7-fold coordination geometry. The coordination sphere around this atom can be considered as being derived from a neodymium-centered octahedron with one of the vertices replaced by two sulfur atoms. As shown in Figure 3c, the neodymium atom is displaced from the center of the equatorial plane, which is presumably due to the uneven bond interactions of opposite sides of the equatorial plane. The single Nd(3)–S(6) bond distance on one side, 2.902 (3) Å, is longer than Nd(3)–S(2) and Nd(3)–S(4) on the other, 2.893 (2) and 2.792 (2) Å,

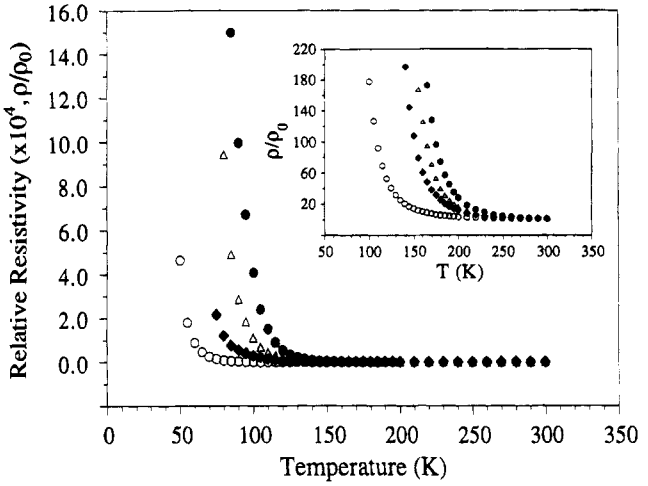

Figure 4. Relative resistivity (ϱ/ϱ_0) vs temperature (kelvin) plot of single crystals of $(RE)_6InTiS_{12}$ (RE = Nd (solid circles), Sm (open triangles), Gd (solid diamonds)) and Gd_3TiS_6 (open circles). The insert shows the blown-up curves of the region at $T \geq 100$ K (see text).

respectively. Regardless of the distortion, the average Nd(3)–S distance, 2.85 Å, is closely comparable with the sum of Shannon crystal radii, 2.866 Å, of the 7-coordinated Nd^{3+} (1.186 Å) and 6-coordinated S^{2-} (1.70 Å). It is noted that the above-described NdS_7 coordination geometry has been observed in a wide range of rare-earth containing phases, *e.g.*, $La_{10}Er_9S_{27}$,[26a] Eu_2BiS_4,[26b] La_3InS_6,[6] Sm_3InS_6,[7] $Tb_3In_5S_{12}$,[8] and $LaPbCuS_3$.[26c]

Electrical Properties. The title compounds present the first structural evidence of an isolated $[TiS_4]_\infty$ infinite chain embedded in a quasi-one-dimensional framework. Electrical properties were examined along the chains of the indexed single crystals mentioned in the Experimental Section. The results of the variable-temperature (T), four-probe resistivity (ϱ) studies are shown in Figure 4. The relative resistivity ϱ/ϱ_0 curves are plotted for T from 300 to 50–85 K, the lowest temperatures at which the resistivity data were acquired. The insert shows blown-up curves in the temperature range of 100–300 K. The room-temperature resistivity is estimated by using the equation described previously,[22] e.g., 1.9, 3.1, 8.3, and 0.094 Ω cm, respectively. The higher resistivity of Gd_6InTiS_{12} compared to Gd_3TiS_6 is attributed to reduced number of $[TiS_4]_\infty$ chains and to the possibility of In^{3+}-ion blocking centers on the $[TiS_4]_\infty$ chains of Gd_6InTiS_{12}. The $\ln(\varrho/\varrho_0)$ vs $1000/T$ plots in Figure 5 are nearly linear, which suggest a semiconducting property. The activation energy (E_a, eV) is calculated from the slope of each linear fit line according to the equation $\ln(\varrho/\varrho_0) = E_a/2kT$, where $k = 8.61739 \times 10^{-5}$ eV K^{-1}. The resulting energies are 0.28, 0.25, 0.22, and 0.14 eV, respectively. Figure 6 shows a nearly linear relationship between the calculated E_a and d_{Ti-Ti} (Å), the distance across the shared octahedral edge of the $[TiS_4]_\infty$ chain.

Considering a model of discrete octahedrally coordinated titanium, a qualitative band structure for a perfect $[TiS_4]_\infty$ octahedral chain can be derived from e_g and t_{2g} orbitals (Figure 7). For simplicity, no further

(26) (a) Carré, D.; Laruelle, P. *Acta Crystallogr.* **1973**, *B29*, 70. (b) Lemoine, P.; Carré, D.; Guittard, M. *Acta Crystallogr.* **1982**, *B38*, 727. (c) Brennan, T.; Ibers, J. A. *J. Solid State Chem.* **1992**, *97*, 377.

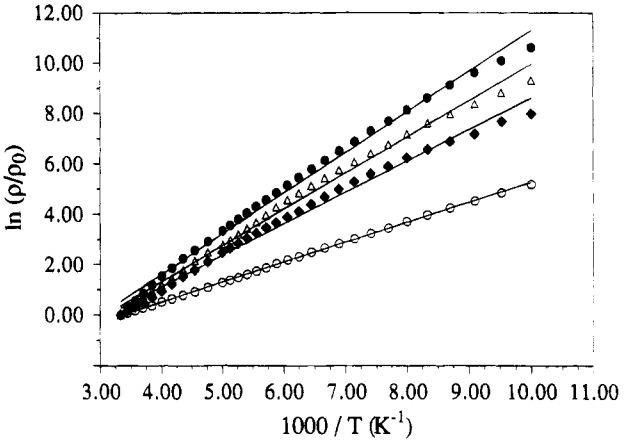

Figure 5. $\ln(\varrho/\varrho_0)$ vs $1000/T$ (K^{-1}) plots of $(RE)_6InTiS_{12}$ (RE = Nd, Sm, Gd) and Gd_3TiS_6. (Same labeling as in Figure 4.) The linearity of the data is demonstrated by the best-fit lines shown.

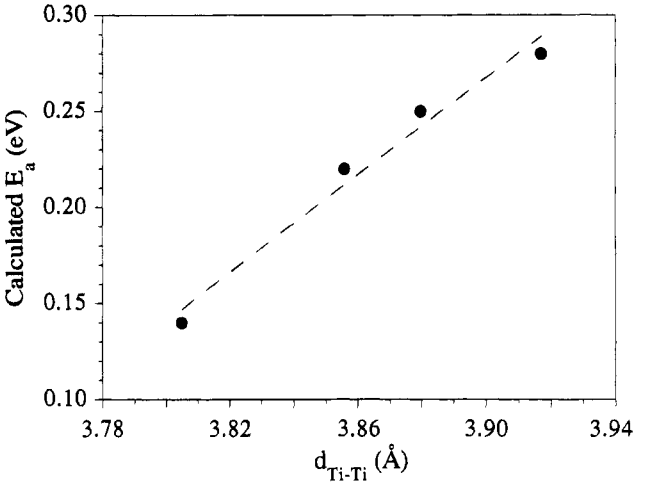

Figure 6. Activation energies (E_a, eV) vs d_{Ti-Ti} ($\equiv c$, Å) plot. The distances used here are from indexed c constants for $(RE)_6InTiS_{12}$ (RE = Nd, Sm, Gd) and Gd_3TiS_6. The broken line indicates the linear fit of the plot.

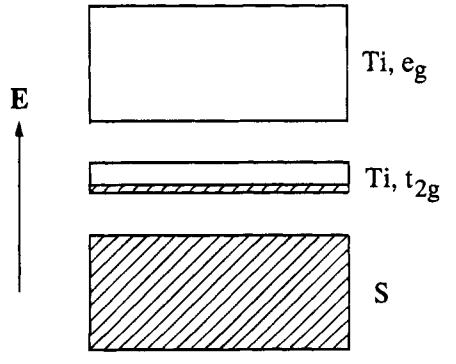

Figure 7. Qualitative band structure for an idealized $[TiS_4]_\infty$ chain. The narrow band in the middle is composed of t_{2g} set of Ti 3d orbitals and is 1/6 filled; see text.

attempt is made to split the Ti t_{2g} orbitals that may correspond to the lowered site symmetry and/or the correlation with the Ti^{4+}/Ti^{3+} and Ti^{3+}/Ti^{2+} couples. Characteristically, the e_g and t_{2g} orbitals are antibonding with respect to the Ti–S bonds, and these orbitals lie higher in energy than s and p orbitals of sulfur atoms.[27] As shown in Figure 7, the "d-block" band made of t_{2g} orbitals is relatively narrow due to a less dispersive bonding nature with respect to the Ti–Ti interaction

along the chain.[28] According to this "phenomenological" model consisting of partially occupied ($^1/_6$) low-lying orbitals, the corresponding phases are predicted to be metallic. However, electrical property analyses show a simple semiconducting behavior with a slight departure toward an insulating state at low temperatures. This phenomenon may be considered as a suppressed M−I transition, commonly observed in 1D materials whose partially filled band at the Fermi level is narrow.[29] Since d_{Ti-Ti}, ca. 3.92 Å, is significantly longer than the critical distance for Ti−Ti interaction, 3.02 Å,[30] a scenario is envisioned involving a regular titanium chain with one discrete electron per site. To investigate the nature of the electronic behavior, a Nd_6InTiS_{12} single-crystal was indexed by X-ray diffraction methods as a function of temperature.[31] The c constant is expected to double if the insulating state is due to electron pairing between adjacent Ti^{3+} sites. However, the indexed unit-cell constants are similar at both 296 and 100 K, indicating no Peierls distortion. Thus, we propose that the on-site repulsion (i.e., the pairing energy) at a Ti^{3+} site dominates over the orbital energy lowering resulting from the interaction between adjacent Ti^{3+} sites. In this situation, a magnetic insulating state of a partially filled band may account for the increased resistivity. To confirm this suggestion, it is necessary to grow large crystals to ensure the In/Ti stoichiometry and measure the magnetic susceptibility as a function of temperature. Detailed band structure calculation with the extended Hückel tight-binding (EHTB) method and high-temperature electrical property measurements would be helpful to reveal the origin of electronic behavior.

Closing Remarks

Synthetically, although an extensive investigation has not been carried out, the title compounds are expected to form a solid solution series as is indicated by the wide range of In/Ti nonstoichiometry, anywhere from 37% to 93% Ti-atom substitutions based on single-crystal studies. The edge-shared $[TiS_4]_\infty$ chain is different than the face-shared 1D chains reported in the MQ_3 and $(MQ_4)_nX$ families in the sense of interchain connectivity. The parallel rutile-like chains are structurally interconnected through Nd−S bonds, which may give rise to a relatively rigid quasi-1D framework and the subsequent absence of Peierls distortion. The Ti−Ti separation distance across the shared edge is dictated by the size of RE^{3+} cations, which facilitates a mechanism for fine tuning associated electronic properties. It should be noted that the observed electrical properties are complicated by the In-atom substitutions (8%−46%) in the $[TiS_4]_\infty$ chain. Experiments to grow sizable single crystals of pure $(RE)_3TiS_6$ phases for the structure/property study are necessary.

Acknowledgment. Financial support for this research from the Robert A. Welch Foundation is gratefully acknowledged. The support for single-crystal X-ray diffractometer and the four-probe resistivity apparatus by the National Science Foundation and Exxon Education Foundation is also acknowledged. The authors are indebted to Mr. M. L. Pierson and Dr. J. C. Stormer, Jr., for microprobe analysis. Suggestions and comments made by referees concerning the interpretation of electrical properties are appreciated.

Supporting Information Available: Tables of detailed crystallographic data, anisotropic thermal parameters, bond distances, and angles are available (15 pages). Ordering information is given on any current masthead page.

CM9501325

(27) (a) The relative energy levels of orbitals in question are based upon H_{ii} (eV) values reported in the literature, *e.g.*, −10.8 eV for Ti (3*d*), −20.0 eV for S (3*s*), and −13.3 eV for S (3*p*). (b) Wang, S., Hwu, S.-J., Paradis, J. A.; Whangbo, M.-H. *J. Am. Chem. Soc.*, in press. (c) Hughbanks, T.; Hoffmann, R. *J. Am. Chem. Soc.* **1983**, *105*, 1150.

(28) Whangbo, M.-H. In *Crystal Chemistry and Properties of Materials with Quasi-One-Dimensional Structures*, Rouxel, J., Ed.; D. Reidel Publishing Co.: Boston, 1986; p 27 and references therein.

(29) (a) Whangbo, M.-H. *Acc. Chem. Res.* **1983**, *16*, 95 and references therein. (b) Whangbo, M.-H. *J. Chem. Phys.* **1979**, *70*, 4963.

(30) Goodenough, J. B. *Bull. Soc. Chim. Fr.* **1965**, 1200.

(31) The indexed cell constants for the Nd_6InTiS_{12} crystal are: a = 13.706 (4) Å, b = 16.272 (7) Å, c = 3.916 (2) Å, V = 873.3 (6) Å^3 at 296 K and a = 13.685 (3) Å, b = 16.251 (5) Å, c = 3.9031 (7) Å, V = 868.0 (3) Å^3 at 100 K.